Intrastrand Cross-Linked Actin between Gln-41 and Cys-374. I. Mapping of Sites Cross-Linked in F-actin by *N*-(4-azido-2-nitrophenyl) Putrescine

György Hegyi,[‡] Marianna Mák,[§] Eldar Kim,[||] Marshall Elzinga,[⊥] Andras Muhlrad,[||,#] and Emil Reisler*,[||]

Department of Biochemistry, Eötvös Lorand University, H-1088 Budapest, Hungary, Spectroscopic Research Division, Gedeon Richter Ltd., Budapest, Hungary, Department of Chemistry and Biochemistry and the Molecular Biology Institute, University of California, Los Angeles, California 90095, and New York State Institute for Basic Research in Developmental Disabilities, New York 10314

Received May 29, 1998; Revised Manuscript Received September 24, 1998

ABSTRACT: A new heterobifunctional photo-cross-linking reagent, *N*-(4-azido-2-nitrophenyl)-putrescine (ANP), was synthesized and covalently bound to Gln-41 of rabbit skeletal muscle actin by a bacterial transglutaminase-mediated reaction. Up to 1.0 mol of the reagent was incorporated per mole of G-actin; at least 90% of it was bound to Gln-41 while a minor fraction (about 8%) was attached to Gln-59. The labeled G-actin was polymerized, and the resulting F-actin was intermolecularly cross-linked by irradiation with UV light. The labeled and cross-linked peptides were isolated from either a complete or limited tryptic digest of cross-linked actin. In the limited digest the tryptic cleavage was restricted to arginine by succinylation of the lysyl residues. N-terminal sequencing and mass spectrometry indicated that the cross-linked peptides contained residues 40−50 (or 40−62 in the arginine limited digest) and residues 373−375, and that the actual cross-linking took place between Gln-41 and Cys-374. This latter finding was also supported by the inhibition of Cys-374 labeling with a fluorescent probe in the cross-linked actin. The dynamic length of ANP, between 11.1 and 12.5 Å, constrains to that range the distance between the γ-carboxyl group of Gln-41 in one monomer and the sulfur atom of Cys-374 in an adjacent monomer. This is consistent with the distances between these two residues on adjacent monomers of the same strand in the long-pitch helix in the structural models of F-actin [Holmes, K. C., Popp, D., Gebhard, W., and Kabsch, W. (1990) *Nature 347*, 44−49 and Lorenz, M., Popp, D., and Holmes, K. C. (1993) *J. Mol. Biol. 234*, 826−836]. The effect of cross-linking on the function of actin is described in the companion papers.

According to atomic structure information the actin monomer (G-actin)[1] consists of four subdomains (*1*−*3*). Normal-mode analysis of the actin structure (*4*) predicts considerable movements of subdomains and individual loops in the molecule. Subdomain 2 of actin and its DNase 1 binding loop (residues 38−52) are the most mobile regions of the molecule (*5*−*7*). In the atomic model of F-actin the DNase 1 binding loop is involved in actin-actin contacts (*2*, *8*, *9*). This is consistent with the inhibition of actin polymerization by chemical modification of His-40 (*10*) and by proteolytic cleavage of the loop with subtilisin (*11*) and the *Escherichia coli* A2 strain protease (*12*).

The structure of F-actin is also dynamic, and as indicated by several biochemical and structural studies, the filaments exist in different conformations depending on the bound divalent cations, nucleotides, and proteins. It has been shown by three-dimensional reconstruction of electron micrographs that a bridge of density, arising from a major structural shift at the C-terminus, exists between the two strands of the actin filament in Ca-actin that is absent in Mg-actin (*13*). Also, the orientation of subdomain 2 depends on the nature of the filament-bound nucleotides and divalent cations (*5*). The tightly bound divalent cation and addition of KCl influence the proteolytic susceptibility of F-actin at subdomain 2 and near the C-terminus (*14*). The structure of F-actin was found to be profoundly affected also by the phosphate analogue BeF_x, which according to Orlova and Egelman (*5*) shifts the position of subdomain 2 to a lower radius in the actin filament. This structural change was also indicated by the BeF_x−induced inhibition of proteolytic cleavage in subdomain 2 of F-actin (*7*).

The basic physical properties of actin filaments were studied extensively by Oosawa and colleagues (*15*). According to them, the filament flexibility is important in the contractile process. During contraction the monomers may change conformation and rotate around the filament axis (*16*, *17*). In view of these studies and the implied functional importance of dynamic changes in F-actin, it is of consider-

[†] This work was supported by grants from Hungarian National Research Fund OTKA T 023618 (to G.H.) and OTKA T 019306 (to M.M.), and the USPHS AR 22031 and NSF MCB-9630997 grants (to E.R.)

[‡] Eötvös Lorand University.

[§] Gedeon Richter Ltd.

[||] University of California

[⊥] New York State Institute for Basic Research in Developmental Disabilities.

[#] Permanent address: Department of Oral Biology, Hebrew University Hadassah School of Dental Medicine, Jerusalem 91120, Israel.

[1] Abbreviations: ANP, *N*-(4-azido-2-nitrophenyl) putrescine; ABP, *N*-(4-azidobenzoyl) putrescine; CMP, 7-diethylamino-3-(4-maleimdylphenyl)-4-methyl coumarin; pPDM, *N*,*N*′-*p*-phenylenebismaleimide; PTH, phenylthiohydantoin; TGase, Ca^2-independent bacterial transglutaminase; G-actin, monomeric actin; F-actin, filamentous (polymerized) actin; ANP-actin, ANP-labeled actin.

10.1021/bi981285j CCC: $15.00
Published on Web 12/05/1998

able interest to determine whether flexibility restrictions affect the physiological properties of actin filaments. One way to decrease the flexibility and perturb inter-monomer motions in F-actin is by chemical cross-linking of adjacent monomers. Intermonomer cross-linking of actin has been performed before using glutaraldehyde (*18*), *p*-phenylenebismaleimide (pPDM) (*19*), dissucininimidyl suberimidate (*20*), and *N*-(4-azidobenzoyl) putrescine (ABP) (*21*). The sites of cross-linking were mapped only for the more specific reagents, pPDM (*22*) and ABP (*21*), from Lys-191 to Cys-374, and from Gln-41 to Lys-113, respectively. The interstrand pPDM cross-linking does not affect the actin activation of myosin ATPase (*23*) or the sliding of actin filaments in standard motility assays. However, the sliding of actin is strongly inhibited by the glutaraldehyde cross-linking of actin (*20*). The effect of the intrastrand ABP cross-linking of F-actin on its functional properties was not studied yet.

The main advantage of the ABP actin cross-linking, besides its high specificity, is that it involves Gln-41 in the DNase binding loop on subdomain 2. This loop is important in actin−actin contacts (*2*, *8*), and the cross-linking offers a way to test the functional significance of its structural transitions. (*5*, *9*).

In this work we used a variant of ABP, a heterobifunctional photo-cross-linking reagent, *N*-(4-azido-2-nitrophenyl) putrescine (ANP). ANP has two advantages over ABP: the efficiency of the photoactivation is improved, and the detection of the colored cross-linking reagent is easier than that of the radioactive label. Moreover, in this work we used a bacterial transglutaminase (*24*), which is also active in the absence of Ca^{2+}. This improves significantly the labeling of Gln-41, which takes place only on monomeric G-actin and is hindered by the slow polymerization of actin in the presence of the millimolar concentration of Ca required for the activity of eukaryotic transglutaminases. Because the length, the properties, and the orientation of the nitrophenyl ring in ANP are different from those in ABP, it was necessary to map the residues cross-linked by ANP in F-actin. We found that ANP cross-links Gln-41 to Cys-374 on two adjacent actin monomers. According to the atomic model of F-actin (*8*, *9*) and the length of ANP, the cross-linked actins must be within the same strand of the long-pitch helix. The functional properties of the cross-linked filaments and the implications of the cross-linking to actomyosin interactions are described in the subsequent two papers.

MATERIALS AND METHODS

Reagents. 7-Diethylamino-3-(4′-maleimidylphenyl)-4-methyl coumarin (CPM) was purchased from Molecular Probes. Putrescine, trypsin (TPCK-treated), carboxypeptidase A, and ATP were obtained from Sigma Chemical Co. 4-Fluoro-3-nitrophenyl azide was from Pierce. Silica Gel 60 was a Merck product. All other reagents were analytical grade: acetonitrile was a SERVA HPLC grade.

Proteins. Actin was isolated from an acetone powder of rabbit skeletal muscle according to the methods of Spudich and Watt (*25*). Ca^{2+}-independent bacterial transglutaminase (TG-ase) was a generous gift of Dr. K. Seguro, Ajimoto, Co., Inc. Japan.

Synthesis of the Cross-Linking Reagent. Synthesis of *N*-(4-azido 2-nitrophenyl) putrescine, ANP, (Figure 1) was similar

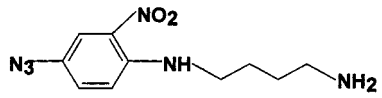

FIGURE 1: The structure of *N*-(azido-2-nitrophenyl putrescine (ANP). The length of the cross-linking reagent, as determined by using the MacSparton molecular modeling program by Wave function Inc. (Irvine, CA), was between 11.1 and 12.5 Å.

to the synthesis of analogous compounds described by Gorman and Folk (*26*). 4-Fluoro-3-nitrophenyl azide (0.6 mmol) dissolved in 2 mL of ethanol was slowly added to 2.5 mmol of putrescine dissolved in 5 mL of ethanol containing 6 mmol of triethylamine. The reaction mixture was incubated at 4 °C overnight, after which the solvent was removed in a rotary evaporator. The sample was redissolved in chloroform−methanol−acetic acid (16:4:1), and after removal of the putrescine precipitate, the 4-azido-2-nitrophenyl-putrescine was purified by preparative chromatography using Silica Gel 60 and chloroform−methanol−acetic acid (16:4:1) as the mobile phase. After removal of the solvent in a rotary evaporator, the sample was redissolved and dried three times from ethanol to remove traces of the chromatography solvent. The final product was dissolved in water, distributed in 5−10 μmol portions in Eppendorf tubes, dried in a Speed-Vac evaporator, and stored at −20 °C. The product was homogeneous on C18 reverse-phase HPLC using 0.1% trifluoroacetic acid−acetonitrile mobile phase, and had a characteristic absorption spectrum with maxima at 470 ($E_{470} = 5.4 \times 10^3$) and 260 nm ($E_{260} = 5 \times 10^4$). The overall yield was 48%.

Labeling of G-actin with ANP by TG-ase. Labeling of G-actin with ANP was carried out by incubating 1 μmol (42 mg) of G actin in 20 mL of G-buffer (4.0 mM Tris-HCl, pH 7.6, 0.4 mM ATP, 0.2 mM $CaCl_2$) containing 8 μmol ANP with 6 units of TG-ase at 4 °C overnight. The labeled sample was then polymerized by the addition of 2.0 mM $MgCl_2$ and 50 mM KCl. The resulting F-actin was pelleted by centrifugation at 40 000 rpm for 2 h in a Beckman 55.2 Ti rotor. The orange−red F actin pellet was homogenized in F-buffer (4.0 mM Tris-HCl, pH 7.6, 0.2 mM ATP, 2 mM $MgCl_2$). The incorporation of the label, as measured by its absorption at 470 nm, varied in several independent preparations between 0.7 and 0.95 mol of label/mol of actin.

Photo-Cross-Linking of the Labeled F-actin. The F-actin solution (∼1 mg/mL) was placed in a 600 mL Pyrex beaker covered by a polyethylene wrap; the depth of the solution was about 1 cm. The solution was gently stirred in an ice bath under a constant stream of N_2 for 40 min to eliminate the dissolved O_2. The incorporated label was photoactivated by irradiation of the sample for 6 min by a Model UVGL-58 Minerallight lamp (UVP Inc.), at a distance of about 15 cm, under a constant stream of N_2. After irradiation, 400 μmol of β-mercaptoethanol was added to quench the unreacted arylazido compound.

Reduction, Alkylation, and Tryptic Digestion of the Cross-Linked Actin. Solid urea was added to the photo-crosslinked F-actin solution containing 400 μmol of β-mercaptoethanol to a concentration of 8 M and the sample was stirred for 2 h at 37 °C; 1 mmol of iodoacetamide was then added and allowed to react for 30 min in the dark. The excess iodoacetamide was quenched by adding 2 mmol of β-mercaptoethanol. When tryptic digestions were restricted to the

Arg peptide bonds, lysyl residues were succinylated as described previously (*21*). The cross-linked alkylated actin was dialyzed exhaustively against water. Solid NH_4HCO_3 was then added to a final concentration of 0.5%, and the sample was digested by trypsin (1 wt %) for 8 h at 37 °C. After lyophylization, the digest was redissolved in 1−1.5 mL of 6 M Guanidine-HCl.

Separation of the Tryptic Peptides. Gel filtration chromatography was performed on a Pharmacia Superdex Peptide FPLC column (1 × 30 cm); the mobile phase (0.5% NH_4HCO_3) was delivered by a LKB 2249 pump at a flow rate of 0.6 mL/min. For the reverse phase, HPLC Nucleosil-300 C18 and Nucleosil-300 C4 columns of Machery-Nagel were used with a Hewlett-Packard 1100 binary pump system. For ion exchange chromatography a Pharmacia Resource-S cartridge was used. The absorbance of all peptides (at 220 nm) and that of the nitrophenyl moiety (at 470 nm) of the labeled peptides was monitored simultaneously by using the LKB-Pharmacia VWM 2141 dual wavelength detector. The acquisition and processing of chromotographic data was done using a Chromatography Station program for Windows by Data Apex Ltd. (Prague, Czech Republic).

Sequencing. N-terminal sequencing of the labeled peptides was carried out using an ABI 470 gas-phase seqencer.

Mass Spectrometry and Carboxypeptidase Digestion. Mass spectrometric experiments were performed using a Finnigan MAT 95SQ hybrid tandem mass spectrometer (ICL Version 10.0 data acquisition system). The instrument, equipped with API sources, was used in electrospray ionization mode; the solvent applied was 50:50 MeOH−H_2O with a small percentage of acetic acid. The ions detected here are doubly charged quasi molecular ions $[M + 2H]^{2+}$. The proteolysis with carboxypeptidase A was performed in a 50 mM NH_4HCO_3 buffer solution. The peptide solution (∼ 1 nmol/μL) was mixed with the enzyme dissolved in the same buffer at a weight ratio of 50:1 (substrate−enzyme). After 10−15 min the reaction was stopped by adding 1 μL of 0.5 M HCl or trifluoroacetic acid to the reaction mixture. This solution was then introduced directly into the ESI source of the mass spectrometer (through a loop injection).

CPM Modification of Cys-374 in F-actin. F-actin (5.0 μM) in 5 mM Tris-HCl, pH 7.8, 0.2 mM ATP, and 2 mM $MgCl_2$ was reacted with CPM (5.0 μM) at 22 °C, and the change in the fluorescence intensity of the probe was monitored versus reaction time at 470 nm. The attachment of CPM to actin is associated with a large increase in CPM fluorescence (*7*). The excitation wavelength was set at 387 nm. Maximum values of CPM fluorescence, corresponding to the plateau values of the fluorescence for F-actins with different extents of ANP cross-linking, were determined at the completion of modification reactions. Actin solutions with different extents of cross-linking were prepared by mixing ANP-labeled and unlabeled G-actin at different ratios followed by their copolymerization into F-actin and the photo-cross-linking. The amount of un-cross-linked actin in each sample was determined by SDS−PAGE analysis of the monomer actin bands.

Fluorescence measurements were carried out in a Spex Fluorolog spectrofluorometer (Spex Industries, Inc., Edison, NJ) in 250 μL cuvettes at 22 °C.

Photo-Cross-linking of Ca^{2}- and Mg^{2+}-F-actin. Ca^{2+}- and Mg^{2+}-ANP-labeled G-actin (70% labeled) were prepared according to Orlova and Egelman (*27*). These actins were polymerized by 3.0 mM $CaCl_2$ and 2.0 mM $MgCl_2$ to yield Ca^{2+}- and Mg^{2+}-F-actins, respectively. All steps were carried out in the dark. The photo-cross-linking of Ca^{2+}- and Mg^{2+}-F-actin solutions (1.0 mg/mL) was conducted as described above. Samples of F-actin were cross-linked for different amounts of time and then denatured and examined on SDS PAGE. The progress of cross-linking reactions was measured by monitoring the disappearance with time of the monomer actin band on SDS gels (*28*). The cross-linking of G-actin followed a first-order process and could be described by a single rate constant.

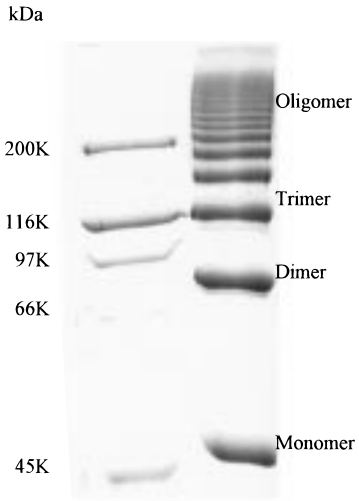

FIGURE 2: SDS−PAGE pattern of cross-linked actin oligomers: 95−100% of ANP-labeled G-actin (∼1 mg/ml) in G-actin buffer (without β-mercaptoethanol) was polymerized by 2 mM $MgCl_2$ and photo-cross-linked by UV irradiation (UV lamp C-62, Ultraviolet products Inc., San Gabriel, CA) for 7 min under N_2 flow. The cross-linked F-actin (right lane) was examined on a 7.5% SDS−PAGE. Molecular weight markers are shown in the left lane. The indicated masses (in kDa), 200, 116, 97, 66, and 45, correspond to myosin, *p*-galactosidase, phosphorylase b, bovine serum albumin, and ovalbumin, respectively. The electrophoretic mobility of ANP cross-linked actin dimer is similar to that of "lower dimer" in the pPDM cross-linked actin (*38*).

SDS−PAGE. SDS gel electrophoresis was performed on 7.5% linear slab gels. Molecular masses of protein bands were estimated by comparing their electrophoretic mobility to that of molecular weight standards.

RESULTS

Cross-Linking of ANP-Labeled F-actin. Bacterial transglutaminase was found to catalyze the ANP labeling of Gln-41 on G-actin with the final yield of labeling approaching 95% or 100% in analytical small-scale tests and between 75% and 85% in large-scale preparations. The extent of F-actin cross-linking, after the polymerization of ANP-G-actin and the photoactivation of the azido group, and the relative amounts of the resulting cross-linked actin oligomers varied somewhat from preparation to preparation even when using the same experimental conditions and similarly labeled G-actin. Figure 2 shows an SDS−PAGE pattern of a representative cross-linking experiment in which the cross-linked actin oligomers are clearly resolved up to a hexamer; the un-cross-linked actin monomers are about 13% of the total actin. More extensive cross-linking leads to a shift of products toward higher oligomers and the disappearance of un-cross-linked actin monomers.

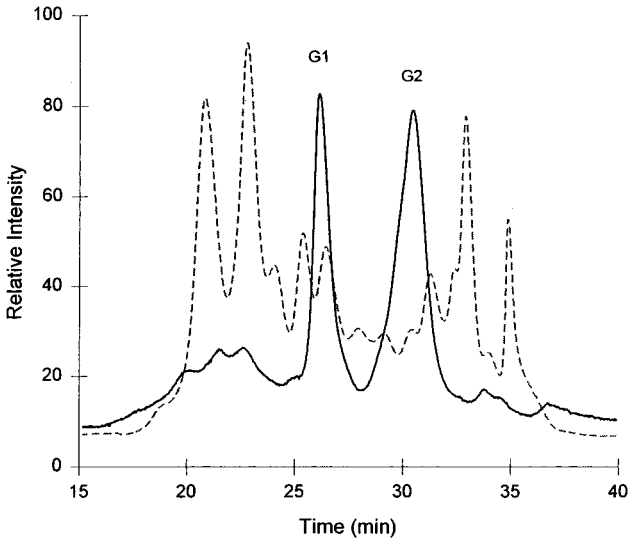

FIGURE 3: Gel filtration of tryptic digest of the photo-cross-linked actin. The filtration column was a Pharmacia Superdex Peptide, and the mobile phase was 0.5% NH_4HCO_3. The flow rate was 0.6 mL/min. The sample was applied to the column in 6 M Guanidine-HCl, and the injected volume was 250 μL. The absorbances were measured at two wavelengths simultaneously. The dashed line profile shows the absorbance of the peptide material at 220 nm AUFS: 3.0; the solid line profile shows the absorbance of the nitrophenyl moiety of the cross-linking reagent at 470 nm AUFS: 0.3. Two colored fractions, G1 and G2, were collected.

Mapping of Cross-Linked Sites: General Strategy. Our mapping strategy is based on the earlier finding that transglutaminase incorporates amines selectivity into Gln-41 of actin; this reaction establishes one of the sites of the cross-linking (*21*, *29*, *30*).

First, the labeled and cross-linked actin was digested by trypsin. Two digests were done, one a complete digest, and a second in which digestion was limited to arginine by succinylation of the lysines. The resulting peptides were resolved by gel filtration and reverse-phase HPLC; the labeled peptides were identified by ANP absorbance. The isolated, labeled peptides were analyzed by N-terminal sequencing and mass spectrometry. The labeled and cross-linked peptide gave a double sequence showing the sequences of the peptides that were cross-linked. Mass spectrometry was also used to identify the labeled and cross-linked peptides.

Isolation of the Labeled and Cross-Linked Peptides. The labeled and photo-cross-linked F-actin was reduced and carboxymethylated prior to digestion by trypsin. The digests were subjected to gel filtration on a Pharmacia Superdex Peptide FPLC column. The elution profiles were monitored simultaneously at 220 and 470 nm to reflect the total peptides and the nitrophenyl-labeled peptides, respectively (Figure 3). Two peptide peaks with absorption in the visible region (G1 and G2) were collected, lyophilized, and further purified. About 40% of the label was found in the G1 fraction and 60% in the G2 fraction. The G-1 peak was then resolved by HPLC (Figure 4). Several peaks were recorded at 220 nm, but only one significant peak was detected at 470 nm at an elution time of 16.2 min. This peak corresponded to a shoulder of an asymmetric peak of 220 nm absorption, indicating that this fraction contains unlabeled peptides as well. This fraction, named G1R1, was collected and rechromatographed using a cation exchange cartridge (Pharmacia Resources-S) in 20 mM Tris-HCl and eluted with a NaCl gradient. The labeled peptide emerged at 85 mM NaCl. Finally, the peptide was chromatographed on a Nucleosil-300 C4 column using a 0.1% TFA−acetonitrile gradient (0−30%). The purified peptide which emerged at 12% acetonitrile was analyzed by MS.

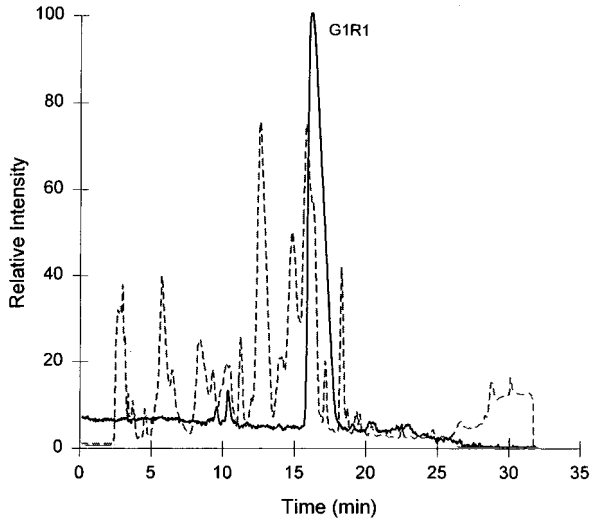

FIGURE 4: Chromatography of peak G1 from Figure 3 on the Nucleosil-300 C18 column. TFA (0.1%) and a linear gradient of 10−40% acetonitrile were used as a mobile phase. The flow rate was 1 mL/min. Absorbances were detected at two wavelengths simultaneously. The dashed line profile shows the absorbance of the peptide material at 220 nm AUFS: 1.0, and the solid line profile shows the absorbance of the nitrophenyl moiety of the cross-linking reagent at 470 nm AUFS: 0.2. One colored fraction, G1R1, was collected.

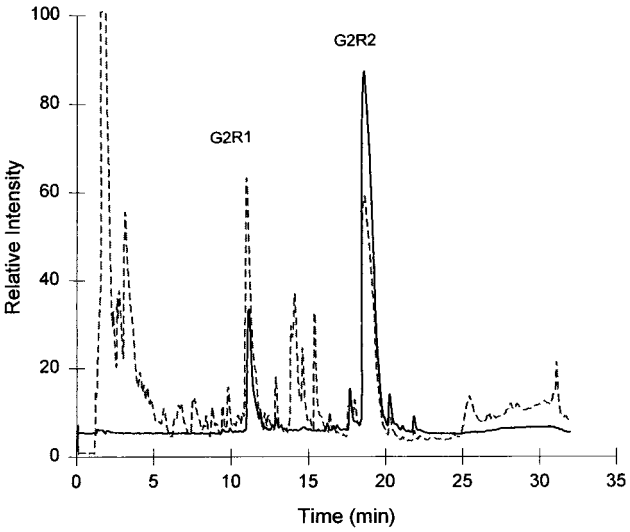

FIGURE 5: Chromatography of peak G2 from Figure 3 on Nucleosil-300 C18 column. TFA (0.1%) and a linear gradient of 10−40% acetonitrile were used as a mobile phase. The flow rate was 1 mL/min. Absorbances were detected at two wavelengths simultaneously. The dashed profile shows the absorbance of peptides at 220 nm AUFS: 1.0, and the solid profile shows the absorbance of the nitrophenyl moiety of the cross-linking reagent at 470 nm AUFS: 0.2. Two colored fractions, G2R1 and G2R2, were collected.

The G2 fraction was also purified on a Nucleosil-300 C18 column (Figure 5). Two peaks showed visible absorption, G2R1 (about 13% of the label) and G2R2 (about 78%). Small amounts of the label were distributed among several other minor peaks. The two selected fractions were rechromato-

graphed on a Nucleosil-300 C4 column with TFA−acetonitrile gradient (0−30%), and the purified peptides were characterized by sequencing and mass spectrometry.

The peptides obtained from the tryptic digest in which cleavage was restricted to arginine (see above) were also separated by FPLC and HPLC as described above (results not shown). The labeled AR1, AR2, AR3, AR4, and AR5 peptides were isolated and analyzed by N-terminal sequencing.

Sequencing of the Isolated Peptides. Several of the labeled peptides were subjected to amino acid sequence analysis. Four different patterns were observed. The first pattern, seen with peptides AR1, AR2, and AR3, which were isolated from the arginine digest of actin in which the lysines were blocked, provided strong evidence for a cross-link between Gln-41 and Cys-374. At step one, PTH-His and PTH-succinyl-Lys were observed in nearly equal amounts. PTH-succinyl-Lys emerges from the HPLC columns between PTH-His and PTH-Ala (*21*). At step two, no identifiable PTH-amino acids were observed. However, two novel peaks were detected, one emerging between PTH-Pro and PTH-Val, and the other about 1 min before PTH-Trp. These peaks probably represent PTH derivatives of the aduct of ANP bound to Gln-41 and cross-linked to the S atom of Cys-374, or perhaps degradation products of this adduct. At step three, PTH-Gly and PTH-Phe were observed, and in subsequent steps the PTH derivatives expected for Val-43 and beyond (Met, Val, Gly, Met, Gly, Gln, Succinyl-Lys, and Asp) were seen. The His and Gly of steps 1 and 3, as well as steps 4−12 correspond to actin residues 40−51, while the Succ-Lys and Phe seen in steps 1 and 3 correspond to actin residues 373 and 375. Thus, the data are completely consistent with the coupling of peptide 40−62 to peptide 373−375 through the side chains of Gln-41 and Cys-374, but we were unable to definitively identify the actual Gln-41-Cys-374 adduct.

The second pattern (results not shown) was seen with peptide AR4. This peptide gave a single sequence beginning at His-40. However, at step 2 (Gln-41), no PTH-Gln was seen, but an unknown peak appeared at a position between PTH-Pro and PTH-Val, at the same position as one of the peaks seen at step 2 of the sequence analysis of peptide (AR1) (see above). This peak is probably Gln-41 bound to ANP and subsequently modified as a result of photolysis, with the azido group converted to an amino group, or perhaps coupled to a constituent of the solvent in which the reaction took place.

A third pattern (results not shown) was seen with peptide AR5. With this peptide, no signal was seen in steps 1 and 2, while steps 3 onward were Gly-42 and subsequent amino acids. This peptide was clearly not cross-linked to another peptide, and a possible explanation for the absence of both His-40 and Gln-41 is that the ANP bound to Gln-41 was cross-linked to the imidazole ring of His-40, and that the hypothesized product after two steps of Edman degradation, PTH-His-40−cross-linker−PTH-Gln-41, did not emerge from the HPLC column of the sequencer during the time used by the sequencer for analysis of PTH-amino acids.

The fourth pattern (results not shown) was seen with peptide G2R1 isolated in low yield from a complete tryptic digest. It gave a sequence that began at Asp-51 and, thus, presumably represented residues 51−60. The only Gln in this sequence, Gln-59, is apparently partially labeled, but there is no evidence that it is cross-linked to another amino acid side chain. Although we observed this result only in a complete (Lys plus Arg) digest of actin, we would not have seen it in the Arg digest because peptide 51−60 would have been part of a larger peptide extending from 40 to 60, itself labeled at Gln-41.

The overall results suggest the following picture. The major site of labeling is Gln-41, and a minor site is Gln-59. Photolysis of the label on Gln-41 results in three possible reactions. The first, and most predominant, is a reaction of the activated cross-linker (perhaps a didehydroazepine (*21*)) with the suflur atom of Cys-374. The second is the reaction of the activated cross-linker with the imidazole moiety of His-40, and the third is the reaction with water or with another component of the solvent.

We do not know exactly what combinations of Gln, Cys, and/or cross-linker were released at step 2 of the first and second patterns described above and therefore cannot be certain of all the chemical reactions taking place. But the fact that a "double sequence", beginning at His-40 and Lys-373, was observed indicates that peptides 40−62 and 373−375 were cross-linked, and the presence of PTH-succ-Lys at step 2 and PTH-Phe at step 3 leaves only Cys-374 as the site of cross-linking. The results of mass spectrometry and fluorescent labeling of Cys-374, as reported below, support the foregoing conclusion.

Mass Spectrometry of the Isolated Peptides. As shown by the mass spectrum in Figure 6A the calculated mass of the G1R1 peptide is 1771. This value is the sum of the masses of the tryptic actin peptide His-40-Lys-50 (1171), the mass of the cross-linking reagent (206), and the mass of the C-terminal tripeptide Lys-373-Phe-375 (396) of actin reduced by the mass of two protons which are lost in the cross-linking reaction. To determine which residue in the Lys-373-Phe-375 tripeptide is cross-linked to the His-40-Lys-50 peptide, we treated the G1R1 peptide with carboxypeptidase A and measured the mass of the truncated peptide again (Figure 6B). The mass of the carboxypeptidase-treated G1R1 is 1624, that is, the enzyme liberates a mass of 147 corresponding to the C-terminal Phe residue. The fact that we did not achieve any further digestion of G1R1 by carboxypeptidase indicates that the photo-cross-linking involves Cys-374 on actin.

Blocking of Cys-374 on actin by ANP photo-cross-linking is also supported by the fact that, in the case of alkylation of actin in 6 M urea by iodoacetamide, the mass data did not show incorporation of the carboxyamino group into the G1R1 peptide, which would be expected if the SH group on Cys-374 would have been free.

The major peptide isolated from the G2 fraction, the G2R2 peptide, has a mass of 1377 (data not shown). This mass originates from the mass of the above-mentioned His40-Lys50 peptide and the mass of the cross-linking reagent (1171 + 206). In this case, as shown by sequencing, ANP was attached to Gln-41 on the peptide but no cross-linking occurred.

The minor labeled component, G2R1, has a mass of 1404. This mass is a sum of the masses of the cross-linking reagent and the Asp51-Lys61 actin tryptic peptide (1198) (data not shown) indicating that Gln-59 is also labeled by TG-ase. However, the distribution of label between the G1 and G2 fractions (40% and 60%, respectively) and the G2R1 and G2R2 peptides (13% and 78%) reveals that only a minor

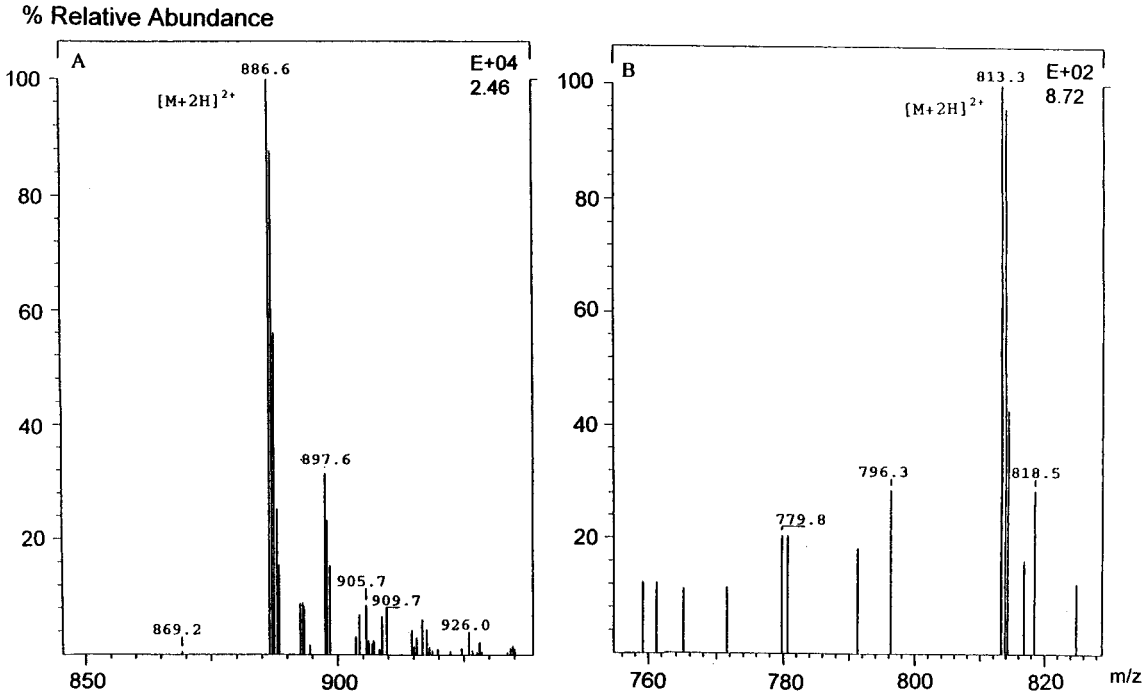

FIGURE 6: Mass Spectra of the G1R1 peptide before (A) and after (B) carboxypeptidase A treatment. The mass spectra were recorded in the electrospray ionization mode, and the ions detected here were the doubly charged quasi molecule ions $[M + 2H]^{2+}$. From Figure 6A, the calculated mass of G1R1 is 1771. From Figure 6B, the calculated mass of the carboxypeptidase-treated G1R1 is 1624. The difference between the two masses is the mass of a Phe residue.

fraction of actin (~8%) is labeled with ANP at Gln-59 by TGase. Moreover, we have not detected any species which might correspond to a peptide cross-linked to the Asp-51-Lys-61 peptide.

Titration of the Cys-374 in F-actin Containing Different Amounts of Photo-Cross-Linked Monomers. The reaction of CPM with Cys-374 on actin, which results in a large increase in CPM fluorescence (*7*), was used to verify the blocking of this residue by the cross-linking reaction. The rationale of this test is that such a blocking should virtually abolish the specific, Cys-374-directed CPM modification of actin. F-actin solutions containing different amounts of un-cross-linked actin were prepared by copolymerizing and photo-cross-linking ANP-labeled and unlabeled G-actin mixed at different ratios. The copolymerized samples were titrated by CPM, and the extent of actin modification at Cys-374 was determined from the final (plateau) fluorescence levels achieved at the completion of these reactions. In Figure 7 the final fluorescence of CPM-actin solutions shows a linear decrease of the CPM modification with a decrease in the amount of un-cross-linked actin. According to these data Cys-374 modification extrapolates to 0 at vanishing concentration of the un-cross-linked monomer. This indicates that the photo-cross-linking and the incorporation of the fluorescent probe compete for the same site, that is, Cys-374, on actin.

Photo-Cross-Linking of ANP-Labeled Ca^{2+}- and Mg^{2+}-F-actin. Structural (*27*) and biochemical (*14*) studies implicated subdamain 2 in the transition between different conformational states associated with the Ca^{2+}- and Mg^{2+}-F-actin filaments. ANP cross-linking of F-actin provides a tool for testing such conformational states of actin. The rates of cross-linking of Ca^{2+}-F-actin and Mg^{2+}-F-actin (polymerized by 3.0 mM $CaCl_2$ and 2.0 mM $MgCl_2$, respectively), which were determined by monitoring the disappearance of

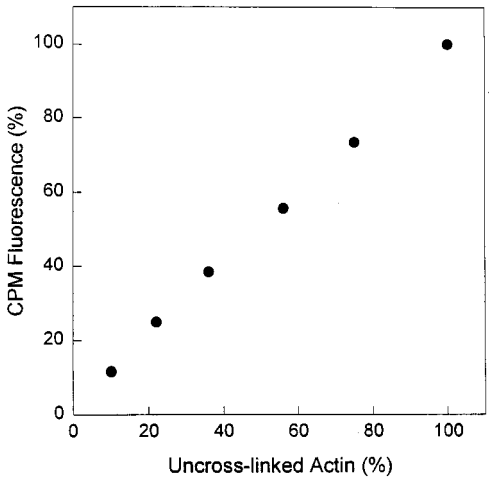

FIGURE 7: CPM modification of F-actin with different extents of ANP cross-linking. Various amounts of unlabeled G-actin were added to 95−100% ANP-labeled G-actin. The resulting mixtures of labeled and unlabeled actins were immediately polymerized by 2 mM $MgCl_2$ and photo-cross-linked as described in Figure 2. CPM modification was carried out as described in Materials and Methods at a 1:1 molar ratio of F-actin and CPM. The amount of un-cross-linked actin monomer in each F-actin solution was determined by SDS−PAGE analysis. The final fluorescence values plotted versus the amount of un-cross-linked actin in each sample correspond to fluorescence plateaus reached at the completion of each reaction. All fluorescence values were corrected for the background fluorescence of free CPM.

un-cross-linked monomer actin band on SDS−PAGE, were indistinguishable from each other. The cross-linking of the two forms of F-actin was described by the same first-order rate constant $k = 0.70 \pm 0.12$ min^{-1}. The extent of cross-linking was also the same for these F-actins. Clearly, ANP cross-linking reactions do not distinguish between the Ca^{2+}- and Mg^{2+}-F-actin.

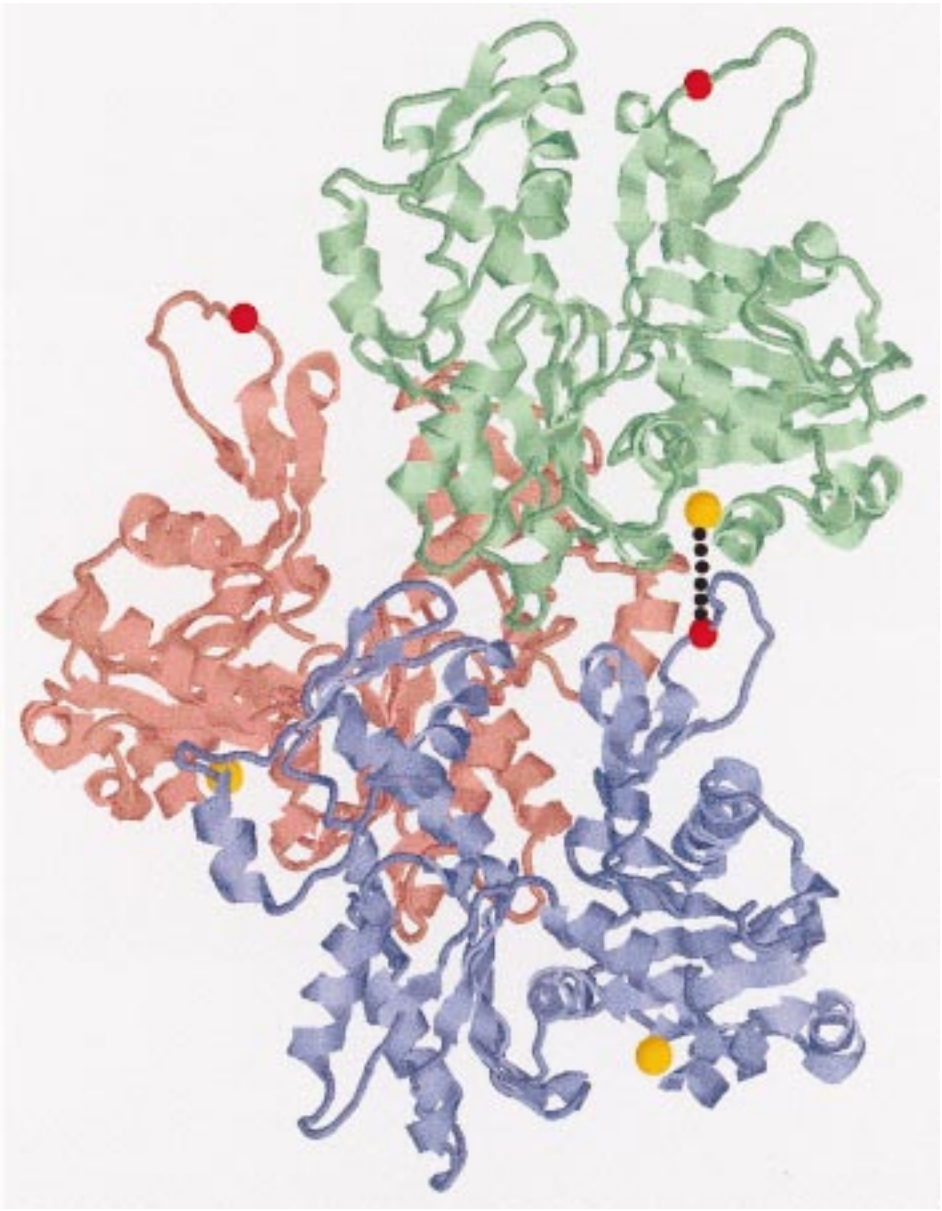

FIGURE 8: The cross-linked residues in the molecular model of F-actin. The molecular model of F-actin is according to Lorenz et al. (*9*). Different actin monomers are represented in blue, green, and pink. Yellow and red spheres are assigned Cys-374 and Gln-41, respectively. The dotted line shows ANP cross-linking between Cys-374 and Gln-41 residues located on neighboring monomers in the same actin strand. The calculated distance between these two residues is 20.7 Å. In the Holmes et al. (*8*) model of F-actin this distance is 12 Å.

DISCUSSION

The ANP cross-linking reagent, whose dynamic length is between 11.1 and 12.5 Å, was found to cross-link the γ-carboxyl group of Gln-41 to the sulfur atom of Cys-374. According to the atomic model of F-actin (*8*, *9*), such a cross-linking must occur between two adjacent monomers of the same strand in the long-pitch helix in F-actin. All other permutations of Cys-374 and Gln-41 cross-linking fall outside of the cross-linking span of ANP. In view of the known flexibility of these regions on actin, the intermolecular cross-linking is consistent with both distances of 12 and 20.7 Å between the two residues (for the α-C atoms), obtained from the molecular models of Holmes et al. (*8*) and Lorenz et al. (*9*), respectively, and agrees with the molecular dynamic refinement of Tirion et al. (*4*) (Figure 8). A possible contact between the DNase binding loop in one monomer and the C-terminus of the adjacent monomer in the same strand of the long-pitch helix was indicated also by the three-dimensional reconstruction of Limulus actin-scruin filament (*31*). We now provide chemical evidence for the close proximity of these two regions.

The high yield and specificity of Gln-41 and Cys-374 cross-linking is somewhat unusual for photoactivated azido-based reactions. Clearly, the specificity of Gln-41 labeling by ANP is due to the TGase. Prior TG-ase-catalyzed labeling of this residue by various alkylamines revealed similar specificity with only a small percentage of probe incorporation to residues other than Gln-41 (*21*, *29*, *30*). The specificity of the second photoactivated reaction is unexpectedly high. This may be due to the rearrangement of the arylazido group after photoactivation to azepine intermediate (*21*), which is a suitable reactive partner for the most nucleophilic group (thiol of Cys-374) in its vicinity. We accounted for about 96% of the labeled tryptic peptides of cross-linked actin, with

approximately 88% identified as Gln-41-labeled and only 8% as Gln-59-labeled peptide. It is not clear whether the latter labeling can also yield cross-linked species; such species have not been detected.

It is quite significant that the ANP cross-linking connects the two most mobile regions of actin. Indeed, the mobility of these regions may even contribute to the high yield of the cross-linking reaction. The dynamic nature of the DNase binding loop, where Gln-41 is located, has been reviewed in the Introduction. In addition, the structure of the second constituent, the C-terminal region, is also highly mobile (*1*) and its conformation changes upon transformation from the Mg to the Ca form of F-actin (*13*). This structural change is manifested in a shift of a bridge of density as seen in the 3-D reconstruction of the filament, and a change in the tryptic susceptibility of the C-terminus. The C-terminal region also has a role in actin−actin contacts and in the integrity of F-actin; it has been shown that removal of the last two or three C-terminal residues destabilizes actin filaments and leads to the appearance of more fragile F-actin in electron micrographs (*32*−*34*). It may seem surprising that the cross-linking rates of Ca^{2+}- and Mg^{2+}-F-actins are identical. However, this result does not necessarily imply, as suggested by Steinmetz et al. (*35*), that the structures of the two types of filaments are similar. It is possible that the presence of ANP on Gln-41 shifts the dynamic equilibrium between conformational states of F-actin and masks the differences between the Ca^{2+}- and Mg^{2+}-actin polymers. Such a possibility is indicated by the effect of another probe attached to Gln-41, dansyl ethylenediamine, on the stability of F-actin (*28*). The effect of ANP on F-actin, if any, must be relatively small; it is undetectable in functional assays of F-actin (paper III in this series), and in subtilisin digestions at loop 38−52 (*11*) in unlabeled and ANP-labeled F-actin (unpublished results).

There is both intra- and intermonomer coupling between the DNase binding loop and the C-terminal region of actin. The intramonomer coupling is allosteric, because of the large distance between the two regions, and works in both directions. DNase I binding to the loop has been shown to introduce a new cleavage site at the distant C-terminus of G-actin (*36*), and the cleavage of the loop between residues 42 and 43 by an actin specific *E. coli* protease was found to affect the spectral characteristics of the fluorescent pyrenyl probe attached to Cys-374 at the C-terminus (*12*). Conversely, when the two last C-terminal residues in Ca-F-actin are cleaved by trypsin, the conformation of subdomain 2 transforms to that observed for Mg-F-actin (*13*).

The intermonomer coupling in actin has been also shown to involve the DNase binding loop and the C-terminus. This conclusion is based on the quenching of the fluorescence of dansyl ethylenediamine attached to Gln-41 by copper bound to Cys-374 in F-actin but not in G-actin and on the increase in proteolytic susceptibility of the loop in F-actin but not in G-actin by the bound copper (*37*). The high mobility of the two regions and the intra- and intermolecular coupling between them are assumed to be essential for the proper functioning of the actin filament. The cross-linking of these regions should significantly decrease their mobility and coupling making the actin−actin contacts more rigid. Functional consequences of such a restriction of motions at the intermolecular interface in F-actin are explored in the two subsequent papers.

REFERENCES

1. Kabsch, W., Mannherz, H.-G., Suck, D., Pai, E., and Holmes, K. C. (1990) *Nature 347*, 37−44.
2. Schutt, C. E., Myslik, J. C., Rozycki, M. D., Goonesekere, N. C. W., and Lindberg, U. (1993) *Nature 365*, 810−816.
3. McLaughlin, P. J., Gooch, J. I., Mannherz, H. G., and Weeds, A. G. (1993) *Nature 364*, 685−692.
4. Tirion, M. M., Ben-Avraham, D., Lopez, M., and Holmes, K. C. (1995) *Biophys. J. 68*, 5−12.
5. Orlova, A., and Egelman, E. H. (1992) *J. Mol. Biol. 227*, 1043−1053.
6. Strzelecka-Golaszewska, H., Moraczewska, J., Khaitlina, S. Y., and Mossakowska, M. (1993) *Eur. J. Biochem. 211*, 731−742.
7. Muhlrad, A., Cheung, P., Phan, B. C., Miller, C., and Reisler, E. (1994) *J. Biol. Chem. 269*, 11852−11858.
8. Holmes, K. C., Popp, D., Gebhard, W., and Kabsch W. (1990) *Nature 347*, 44−49.
9. Lorenz, M., Popp, D., and Holmes, K. C. (1993) *J. Mol. Biol. 234*, 826−836.
10. Hegyi, G., Premecz, G., Sain, B., and Muhlrad, A. (1974) *Eur. J. Biochem. 44*, 7−12.
11. Schwyter, D., Phillips, M., and Reisler, E. (1989) *Biochemistry 28*, 5889−5895.
12. Khaitlina, S. Y., Moraczewska, J., and Strzelecka-Golaszewska, H. (1993*) Eur. J. Biochem. 218*, 911−920.
13. Orlova, A., and Egelman, E. H. (1995) *J. Mol. Biol. 245*, 582−597.
14. Strzelecka-Golaszewska, H., Wozniak, A., Hult, T., and Lindberg, U. (1996) *Biochem. J. 316*, 713−721.
15. Oosawa, F., Fujime, S., Ishiwata, S., and Mihashi, K. (1972) *Cold Spring Harbor Symp. Quant. Biol. 37*, 277−285.
16. Prochniewicz-Nakayama, E., Yanagida, T., and Oosawa, F. (1983) *J. Cell Biol. 97*, 1663−1667.
17. Miki, M., dos Remedios, C., and Barden, J. A. (1987) *Eur. J. Biochem. 168*, 339−345.
18. Gadasi, H., Oplatka, A., Lamed, R., Hochberg, A., and Low, W. (1974) *Biochim. Biophys. Acta 333*, 161−168.
19. Knight, P., and Offer, G. (1978) *Biochem. J. 175*, 1023−1032.
20. Prochniewicz, E., and Yanagida, T. (1990) *J. Mol. Biol. 216*, 761−772.
21. Hegyi, G., Michel, H., Shabanowitz, J., Hunt, D. F., Chatterjie, N., Healy-Louie, G., and Elzinga M. (1992) *Protein Sci. 1*, 132−144.
22. Elzinga, M., and Phelan, J. J. (1984) *Proc. Natl. Acad. Sci. U.S.A. 81*, 6599−6602.
23. Mockrin, S. C., and Korn, E. D. (1981) *J. Biol. Chem. 256*, 8228−8233.
24. Ando, H., Adachi, M., Umeda, K., Matsuura, A., Nonaka, M., Uchio, R., Tanaka, H., and Motoki, M. (1989) *Agric. Biol. Chem. 53*, 2613−2617.
25. Spudich, J. A., and Watt, S. (1971) *J. Biol. Chem. 246*, 4866−4871.
26. Gorman, J. J., and Folk, J. E. (1980) *J. Biol. Chem. 225*, 1175−1180.
27. Orlova, A., and Egelman, E. H. (1993) *J. Mol. Biol. 232*, 334−341.
28. Kim, E., Miller, C. J., Motoki, M., Seguro, K., Muhlrad, A., and Reisler, E. (1996) *Biophys J. 70*, 1439−1446.
29. Takashi, R. (1988) *Biochemistry 27*, 938−943.
30. Kim, E., Motoki, M., Seguro, K., Muhlrad, A., and Reisler E. (1995) *Biophys. J. 69*, 2024−2032.
31. Owen, C., and DeRosier, D. (1993) *J. Cell Biol. 123*, 337−344.
32. O'Donoghue, S. I., Miki, M., and dos Remedios, C. (1992) *Arch. Biochem. Biophys. 293*, 110−116.
33. Mossakowska, M., Moraczewska, J., Khaitlina, S., and Strzelecka-Golaszewska, H. (1993) *Biochem. J. 289*, 897−902.

34. Drewes, G., and Faulstich, H. (1993) *Eur. J. Biochem. 212*, 247−253.
35. Steinmetz, M. O., Goldie, K. N., and Aebi, U. (1997) *J. Cell Biol. 138*, 559−574.
36. Crosbie, R. H., Miller, C., Cheung, P., Goodnight, T., Muhlrad, A., and Reisler, E. (1994) *Biophys. J. 67*, 1957−1964.
37. Kim, E., and Reisler, E. (1996) *Biophys J. 71*, 1914−1919.
38. Millonig, R. C., Salvo, H., and Aebi, U. (1988) *J. Cell Biol. 106*,785−796

BI981285J